J. Membrane Biol. 152, 39–48 (1996)

The Journal of
Membrane
Biology

Sea Anemone Toxin (ATX II) Modulation of Heart and Skeletal Muscle Sodium Channel α-Subunits Expressed in tsA201 Cells

M. Chahine[1], **E. Plante**[1], **R.G. Kallen**[2]

[1]Laval Hospital, Research Center, 2725, Chemin St.-Foy, St.-Foy, Québec, Canada G1V 4G5
[2]Department of Biochemistry and Biophysics, University of Pennsylvania, Philadelphia, PA 19104-6059

Received: 5 December 1995/Revised: 1 March 1996

Abstract. We have expressed recombinant α-subunits of hH1 (human heart subtype 1), rSkM1 (rat skeletal muscle subtype 1) and hSkM1 (human skeletal muscle) sodium channels in human embryonic kidney cell line, namely the tsA201 cells and compared the effects of ATX II on these sodium channel subtypes. ATX II slows the inactivation phase of hH1 with little or no effect on activation. At intermediate concentrations of ATX II the time course of inactivation is biexponential due to the mixture of free (fast component, τ_h^{fast}) and toxin-bound (slow component, τ_h^{slow}) channels. The relative amplitude of τ_h^{slow} allows an estimate of the IC_{50} values ~11 nM. The slowing of inactivation in the presence of ATX II is consistent with destabilization of the inactivated state by toxin binding. Further evidence for this conclusion is: (i) The voltage-dependence of the current decay time constants (τ_h) is lost or possibly reversed (time constants plateau or increase at more positive voltages in contrast to these of untreated channels). (ii) The single channel mean open times are increased by a factor of two in the presence of ATX II. (iii) The recovery from inactivation is faster in the presence of ATX II.

Similar effects of ATX II on rSkM1 channel behavior occur, but only at higher concentrations of toxin (IC_{50} = 51 nM). The slowing of inactivation on hSkM1 is comparable to the one seen with rSkM1.

A residual or window current appears in the presence of ATX II that is similar to that observed in channels containing mutations associated with some of the familial periodic paralyses.

Key words: Sea anemone toxin — Sodium channel — Human heart — Skeletal muscle — Expression — Complementary DNA

Correspondence to: M. Chahine

Introduction

Voltage-gated sodium channels are large, highly secondarily modified transmembrane proteins responsible for the rapid rise of action potentials in excitable cells such as nerve and striated muscle (Kallen et al., 1993; Catterall, 1994).

Voltage-gated sodium channels consist of one α-subunit (~260 kDa 1800–2000 amino acids) and, generally, one or two β-subunits in the 30–40 kDa range (Kallen et al., 1993; Catterall, 1994). The α-subunits encoding different sodium channel subtypes, including those from human heart, (hH1) (Gellens et al., 1992), adult rat skeletal muscle, (rSkM1) (Trimmer et al., 1989), and adult human skeletal muscle, (hSkM1) (George et al., 1992; Wang et al., 1992) have been cloned, sequenced and functionally expressed in *Xenopus* oocytes and mammalian cell lines (chinese hamster ovary, CHO or human embryonic kidney, tsA 201 cells) (White et al., 1991; Krafte et al., 1994; Noda, 1994). The microinjection or transfection of nucleic acid encoding only the α-subunit is sufficient for functional expression of voltage-gated sodium channels (White et al., 1991; Catterall, 1992; Catterall, 1994; Krafte et al., 1994; Noda, 1994). These studies also showed that the α-subunit contains the interaction sites for drugs and toxins known from previous experiments to interact with voltage-gated sodium channels in native tissues.

Toxins have effects on voltage-gated sodium channels that range from pore blocker (e.g., tetrodotoxin, TTX and μ-conotoxin, μ-CTX) to modification of the gating and permeation of these channels (e.g., batrachotoxin) (Catterall, 1992).

Initially, radiolabeled guanidinium toxins (e.g., saxotoxin, STX) were used in the purification of eel *Electrophorus electricus* sodium ion channel proteins which led, ultimately, to the cloning of the gene (Noda et

al., 1984). More recently, TTX and μ-CTX have been used to map the structure of expressed recombinant voltage-gated ion channels (Terlau et al., 1991; Backx et al., 1992; Chen et al., 1992; Satin et al., 1992; Lipkind & Fozzard, 1994; Chahine et al., 1995). Our attention has now shifted to the interactions of polypeptide toxins with channels because the three-dimensional structures of these ligands are currently known or are being determined and the toxins provide very useful probes of channel structure (Torda et al., 1988; Torda & Norton, 1989; Widmer et al., 1989; Wilcox et al., 1993).

The subject of the present study is a sea anemone toxin, ATX II, a 47 amino acid peptide toxin purified from *Anemonia sulcata.* Similar to μ-CTX, ATX II contains three disulfide bridges (Béress et al., 1975*a*,*b*). Previous studies have shown that ATX II and μ-CTX differentially discriminate between TTX-sensitive and TTX-resistant sodium channels of striated muscle and nerve (Vincent et al., 1980; Frelin et al., 1984). Immature and denervated skeletal muscle and heart express a TTX-resistant/μ-CTX-resistant/ATX II-sensitive sodium channel whereas mature skeletal muscle is characterized by the presence of a TTX-sensitive/μ-CTX-sensitive/ATX II-resistant sodium channel (Erxleben & Rathmayer, 1984; Kallen et al., 1993). The effect of higher concentrations of ATX II, measured by voltage clamp methods on mouse skeletal muscle fibers, is to prolong the action potential duration recorded from denervated, but less markedly from normal, skeletal muscle by slowing the inactivation of sodium channels (Romey et al., 1980; Erxleben & Rathmayer, 1984).

ATX II binds preferentially to the open state of cardiac sodium channels (Schreibmayer, Kazerani & Tritthart, 1987) and reduces the rate of inactivation from the open state (El-Sherif, Fozzard & Hanck, 1992). In this sense, the effect of the toxin is similar to that of mutations in the skeletal muscle sodium channel α-subunit that prolong inactivation and are responsible for paralytic diseases of humans (i.e., Paramyotonia Congenita or PC) (Ptácek et al., 1992; Cannon & Corey, 1993; Chahine et al., 1994). The cardiotonic effect of ATX II appears to be related to this slowing of inactivation of sodium channels, (Alsen et al., 1981) which primarily increases sodium influx and secondarily calcium influx via the Na^+-Ca^{2+} exchanger (Romey et al., 1980). A related toxin, Anthopleurin-A (AP-A) was reported to induce an inotropic effect on the myocardium (Shibata et al., 1976) with no apparent effect on the peripheral circulation (mean arterial pressure) (Blair, Peterson & Bishop, 1978).

For drug development it is of importance to know the mechanism by which this toxin slows the inactivation of human cardiac sodium channels. The first step in this process is to further characterize its action and binding site. In this regard, there have been several studies of the interaction site of an α-scorpion peptide toxin from *Leiurus quinquestriatus*. This toxin slows the inactivation of voltage-gated rat brain sodium channels by interacting with a sea anemone toxin receptors on the extracellulare surface of the channel (Hille, 1992). Using competing monoclonal antibodies the binding site of α-scorpion toxin was shown to include the loop connecting the putative fifth and sixth transmembrane segments (S5–S6 loop) of Domains 1 and 4, (Thomsen & Catterall, 1989) suggesting that the related toxin, ATX II, may also interact with S5–S6 loops in Domains 1 and 4.

In this study, we have expressed hH1, rSkM1 and hSkM1 sodium channels by transient transfection in the tsA 201 cell line and examined the effect of ATX II on these isoforms using patch-clamp methods.

Material and Methods

Chemicals and Biochemicals

ATX II, the isoleucine isotoxin from *Anemonia sulcata,* was purchased from Calbiochem-Novabiochem International, San Diego, CA.

tsA201 Cell Line

The tsA201 cell line was kindly provided by Dr. R. Horn (Jefferson Medical College, Jefferson University) and grown in high glucose Dulbecco's Minimal Eagles Medium (DMEM), supplemented with 2 mM L-glutamine, 10% fetal bovine serum and penicillin-streptomycin (Gibco BRL), in 5% CO_2 humid atmosphere incubator.

Cell Transfection

The details of the transient transfection procedure have been described elsewhere (Chahine et al., 1994; Margolskee, McHendry-Rinde & Horn, 1993). Briefly, transfection of tsA201 cells grown to 30–50% confluence on 100 mm plates with 10 mg of channel cDNAs, and 10 mg of salmon sperm DNA (Gibco BRL) as a carrier, utilized the calcium phosphate method. For patch clamp experiments the cells were used 2–3 days after transfection. The coding segment of rSkM1 (Trimmer et al., 1989) or hH1 (Gellens et al., 1992) was cloned into HindIII and Xbal sites of pcDNA I (Invitrogen, San Diego, CA). hSkM1 in pRc/CMV was provided by Dr. A.L. George, (Departments of Medicine and Pharmacology, Vanderbilt University School of Medicine). Plasmid DNA was purified using Qiagen exchange columns (Qiagen, Chatsworth, CA).

Patch Clamp

Patch electrodes were made from Corning 8161 glass and coated with Sylgard (Dow Corning, Midland, MI) to reduce its capacitance. For whole-cell recording the patch pipette contained (mM): 35, NaCl; 105, CsF; 10, EGTA; and 10, Cs-HEPES (pH = 7.4). The bath solution contained (mM): 150, NaCl; 2, KCl; 1.5, $CaCl_2$; 1, $MgCl_2$; 10, glucose; and 10, Na-HEPES (pH = 7.4). For cell-attached experiments the bath solution contained (mM): 100, K-aspartate, 50, KCl; 1.5, $CaCl_2$; 1, $MgCl_2$; 10, glucose and 10, K-HEPES (pH = 7.4). The pipette solution contained (mM): 150, NaCl; 10, tetraethylammonium chloride (to

block endogenous potassium channels); 2, KCl; 1.5, $CaCl_2$; 1, $MgCl_2$; 10, glucose and 10, Na-HEPES (pH = 7.4). Records were obtained using an Axopatch-1B amplifier (Axon Instruments, Burlingame, CA). For whole cell recording a routine > 80% series resistance and capacitance compensation were performed in order to minimize voltage errors. Sodium currents were leak corrected using Axopatch 1-B leak subtraction and filtered at 5 KHz. Data were acquired using the Digidata 1200 acquisition system (Axon Instruments). Data-acquisition, storage and analysis were performed using pClamp (Axon Instruments).

Single Channel Analysis

Single channel records were filtered at 5 KHz and sampled at 100 KHz. For analysis, currents were filtered again using a digital filter at 3.5 KHz and idealized with the TRANSIT program (Dr. A. VanDongen, Duke University). Single channel amplitudes were measured either by hand using the pClamp program or from amplitude histograms using TRANSIT. Mean open times of single channel data were analyzed using a likelihood estimate (Horn & Lange, 1983). Data are presented as mean ± SEM. All experiments were performed at room temperature, 22–23°C.

Results

Effects of ATX II on hH1 and rSkM1

Sodium currents from standard whole cell recordings at two to three days following transfection of tsA201 cells with cDNA encoding hH1 in the absence and presence of 100 nM ATX II are shown in Fig. 1*A* and *B*. The currents were triggered by 30 msec (Control) and 80 msec (ATX II-treated) pulse durations from a holding potential of −100 mV stepped in 10 mV increments to +60 mV.Typical sodium currents in the absence of ATX II exhibit normal fast activation and inactivation kinetics. Inward sodium currents appear at about −70 mV and reach a maximum at −30 mV: at voltages more positive than +35 mV, outward currents are observed. The effect of ATX II (100 nM) on currents obtained at step depolarizations in the voltage range from −100 to −30 mV is to dramatically slow the inactivation rate of hH1 sodium currents (~27-fold at −20 mV, 100 nM ATX II). There are, at best, minor effects of toxin on activation (*see below*). The effect of 100 nM ATX II on a family of rSkM1 currents under comparable conditions shows qualitatively similar but quantitatively different results (Fig. 1*C* and *D*). The currents were triggered by 30 msec (Control) and 55 msec (ATX II-treated) pulse durations from a holding potential of −100 mV stepped in 10 mV increments to +60 mV.

The striking slowing of the inactivation rate of hH1 sodium currents is not accompanied by similar effects on activation kinetics. Normalized traces recorded at high sampling rate (2048-sample segment, with Axopatch 1-B leak subtraction and a frequency filter of 5 KHz) in the presence and the absence of the toxin were superimposed

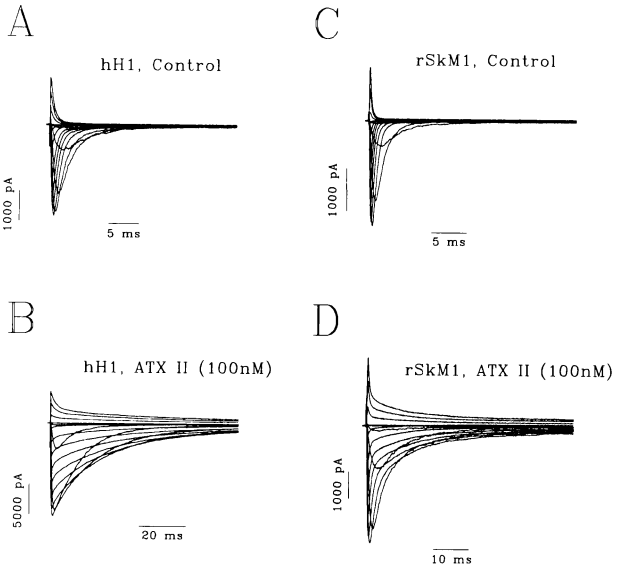

Fig. 1. Effects of sea anemone toxin (ATX II) on human heart (hH1) and rat skeletal muscle (rSkM1) sodium channels. Whole cell sodium currents due to hH1 and rSkM1 sodium channels recorded from transfected tsA201 cell line at a holding potential of −100 mV and stepped from −80 to +60 mV in 10 mV increments. hH1: (*A*) in absence and (*B*) in presence of 100 nM ATX II and rSkM1: (*C*) in absence and (*D*) in presence of 100 nM ATX II. Note the difference in the time scale for hH1 and rSkM1 in presence of the toxin.

and showed that in the presence of the toxin there is little, if any, effect on hH1 activation kinetics (Fig. 2*A* and *C*). The slowing in the rate of inactivation is responsible for the slight increases in the amplitude of the current (Fig. 2*A*). A plot of the peak sodium current as a function of voltage (*I/V*) in the presence of ATX II indicates that the inward sodium current appears at voltages of about −70 mV and maximum current was recorded at −40 mV (Fig. 2*B*). The reversal potential (E_{rev}) was unchanged in the presence of toxin and is consistent with that calculated from the Nernst equation, $E_{rev} = (RT/zF)ln[Na]_o/[Na]_{in}$ = 37 mV, where $[Na]_o$ = 150 mM and $[Na]_{in}$ = 35 mM (Fig. 2*B*).

To study the kinetics of inactivation, the time course of the inactivation phase was fit to a single exponential for hH1 in the absence of toxin and to two exponentials with time constant values, τ_h^{slow} and τ_h^{fast}, in the presence of intermediate concentrations of the toxin. The time constant values at 100 nM ATX II were plotted as a function of voltage (Fig. 3*A*) and show that at −20 mV the value of τ_h^{slow} is increased by ~27-fold. From −40 to +20 mV the slope of the voltage dependence was zero or perhaps somewhat positive (with a tendency for the values of τ_h^{slow} becoming progressively larger at more positive voltages) indicating that the voltage dependence of the time constant of the toxin-treated channels is substantially less than that of untreated channels. At 100 nM ATX II, the effects of toxin on rSkM1 are similar but

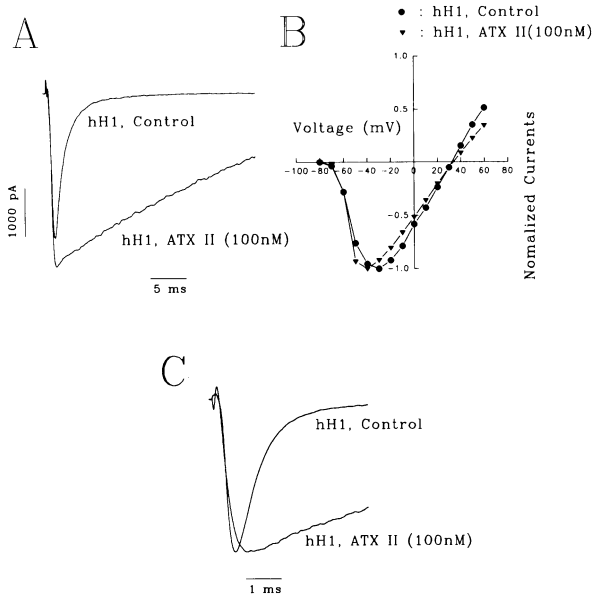

Fig. 2. Effect of sea anemone toxin (ATX II) on the human heart (hH1) sodium channel activation kinetics and on the *I/V* relationship. (*A*) Effects of ATX II on sodium current recorded at −20 mV, stepped from a holding potential of −100 mV. (*B*) Effects of ATX II on the current-voltage relationship (*I/V*) of the experiment shown on *A.* The closed circles represents control *I/V* relationship and the closed triangles represent the *I/V* curve in the presence of ATX II, *I/V* curves were normalized to the maximum current. (*C*) Superimposed currents scaled to equal amplitudes at −20 mV of hH1 in presence and in absence of ATX II at 100 nM recorded at a high sampling rate (2048-sample segment) showing little or no effect on the activation kinetics.

somewhat less remarkable (Fig. 3*E*). On rSkM1, ATX II has no effect on the current-voltage relationship (*data not shown*). The inactivation rate (τ_h^{slow}) is slowed by a factor of 12-fold at −20 mV at 100 nM toxin.

The inactivation of sodium currents in the presence of nonsaturating concentrations of toxin is biexponential for hH1 (Fig.4*A*, *B* and *C*) and rSkM1 (*not shown*). At higher concentrations of toxin, the kinetics of inactivation becomes monoexponential and we have attributed the biexponential behavior of inactivation at intermediate toxin concentrations to the inactivation of free and toxin-bound channels (characterized by time constants, τ_h^{fast} and τ_h^{slow}, respectively) (Fig. 4*C*). We estimate IC_{50} = 11 and 51 nM (Fig. 4*D*) for the effect of ATX II on the hH1 and rSkM1 sodium channels from the toxin concentration dependence of the ratio of the amplitude of the contribution of the slower exponential to the amplitude of total current. These data indicate that rSkM1 is less sensitive to ATX II than hH1, presumably due to the different structures of these two subtypes which are encoded by different genes.

The steady-state inactivation (h_∞) of hH1 in the presence of 100 nM ATX II was studied using a two-pulse protocol with 500 msec prepulse duration and −30 mV test voltage and plotting the amplitude of the current *vs.* the prepulse voltage (Fig. 3*B*). The data points were fit using a Boltzmann equation with midpoints of $V_{1/2}$ = −95.3 ± 7 mV (n = 6) and −92.5 ± 2 mV (n = 4) and slope factors of K_v = 6 ± 0.3 and 8.4 ± 0.1 without and with the toxin, respectively (Fig. 3*B*). Thus, ATX II does not induce a significant shift of the h_∞ curve but does cause a decrease in sensitivity of inactivation to changing voltage. A similar situation obtains for ATX II effects on rSkM1 (Fig. 3*F*).

The recovery of current from inactivation for hH1, measured with a two-pulse protocol at −30 mV with a prepulse duration of 40 msec (control) and 100 msec (in presence of ATX II), follows a single exponential (Fig. 3*C* and *G*). The normalized peak currents of test pulses *vs.* time between the prepulse and the test pulse (Δt) were fit to single exponentials characterized by time constants, τ_{rec}. The rate of the recovery is significantly faster in the presence of 100 nM toxin so that in this case only the latter portion of the reaction was available for analysis. The time constants were 72.3 ± 4 msec (n = 5) and 19.7 ± 1.6 msec (n = 3) at −100 mV holding potential, without and with toxin, respectively, suggesting that the stability of the inactivated state with toxin bound is decreased. rSkM1 shows faster kinetics of recovery from inactivation than hH1 both in the absence and presence of toxin but, more importantly, the effect of toxin on rSkM1 is to increase the rate of recovery from inactivation.

The data points for the voltage-dependence of normalized conductance (steady-state activation or G-V plot), derived from current-voltage relation of hH1 in the absence and presence of 100 nM ATX II were fit using a Boltzmann equation with midpoints of $V_{1/2}$ = −54.6 ± 3 (n = 3) and −54.9 ± 0.6 mV (n = 3) and slope factors of K_v = −3.1 ± 1 and −5 ± 0.5, respectively (Fig. 3*D*). Thus, ATX II does not induce a significant shift of the G-V curve but does cause a decrease in sensitivity of activation to changing voltage. A similar situation obtains for ATX II effects on rSkM1 with values in the absence and presence of 100 nM toxin as follows: $V_{1/2}$ = −35.8 ± 2 mV (n = 3) and −33.1 ± 5 mV (n = 5) and slope factors of K_v = −5.6 ± 2 and −6.44 ± 0.3, respectively (Fig. 3*H*).

Single-Channel Recordings

Single channel recordings were obtained in the cell-attached configuration. To study the effect of ATX II on hH1 at the single channel level, the toxin was added to the patch pipette and gigaohm seals were then completed. Recordings were obtained of single channel currents at −20 mV from a holding potential of −120 mV with a 20 msec test pulse duration (Fig. 5*A* and *B*). Only patches containing 2 to 3 channels were analyzed. ATX

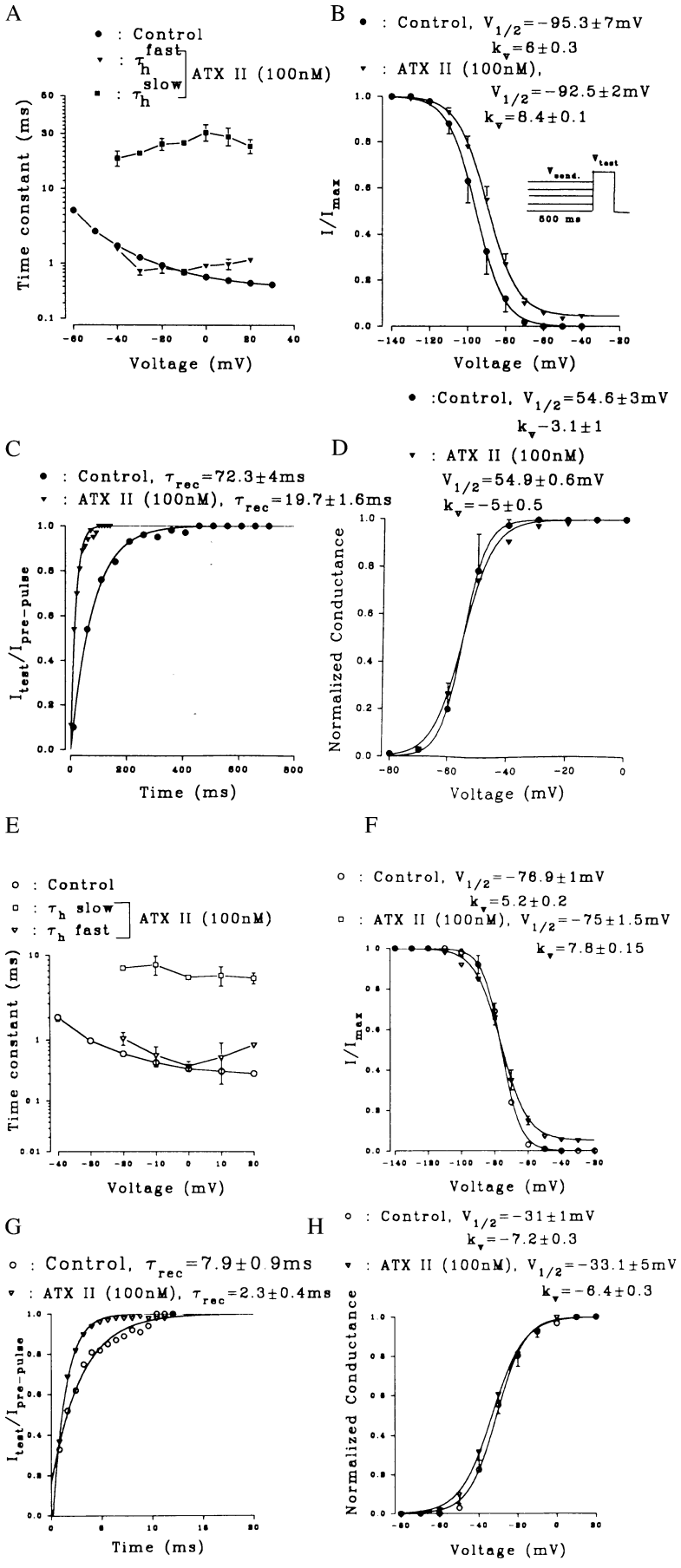

Fig. 3. Effect of sea anemone toxin (ATX II) on the voltage dependence of inactivation (τ_h), *steady-state inactivation (h_∞) and recovery from inactivation (τ_{rec}) of human heart (hH1) (A-D) and rat skeletal muscle rSkM1 (E-H) sodium channels. (A)* Voltage dependence of time constants for inactivation: τ_h, for monophasic kinetics in absence (●, $n = 7$) of ATX II and τ_h^{fast} and τ_h^{slow}, for biphasic kinetics in the presence of the ATX II (100 nM) {▼ and ■, $n = 5$}. (*B*) Steady-state inactivation (h_∞) at −30 mV triggered by 500-msec prepulses at indicated voltages in the absence (●) and presence (▼) of ATX II (100 nM). Data points were fitted using a Boltzmann equation, $I/I_{max} = 1/(1 + \exp\{\{V - V_{1/2}\}/K_v\})$, and half-maximal voltage, $V_{1/2}$, and slope factor, K_v, values in the absence (●, $n = 6$) and presence (▼, $n = 4$) of ATX II (100 nM) as given, where I_{max} is the maximum current measured at a holding potential of −140 mV. (*C*) Recovery from inactivation. Two-pulse protocol with exponential recovery kinetics, measured at −30 mV following a prepulse of 40 msec (control) and 100 msec (in presence of ATX II) at −30 mV (holding potential = −100 mV), fit to the equation, $I_{test}/I_{pre\text{-}pulse} = 1 - \exp\{-t/\tau\}$, where t is the time constant of recovery from inactivation, in the absence (●, $n = 5$) and presence (▼, $n = 3$) of ATX II (100 nM). (*D*) Normalized conductance-voltage for hH1 in presence (▼, $n = 3$) and in absence (●, $n = 3$) of ATX II, fitted with a Boltzmann equation. (*E*) Voltage dependence of time constants for inactivation: τ_h, for monophasic kinetics in absence (○, $n = 4$) of ATX II and τ_h^{fast} and τ_h^{slow}, for biphasic kinetics in the presence of the ATX II (100 nM) {▽, $n = 3$ and □, $n = 3$}. (*E*) Steady-state inactivation (h_∞) at −30 mV triggered by 500 msec prepulses at indicated voltages in the absence (○) and presence (▽) of ATX II (100 nM). Data points were fitted using a Boltzmann equation, $I/I_{max} = 1/(1 + \exp\{\{V - V_{1/2}\}/K_v\})$, and half-maximal voltage, $V_{1/2}$, and slope factor, K_v, values in the absence (○, $n = 5$) and presence (▽, $n = 3$) of ATX II (100 nM) as given in the figure, where I_{max} is the maximum current measured at a holding potential of −140 mV. (*G*) Recovery from inactivation. Two-pulse protocol with exponential recovery kinetics, measured at −30 mV following a prepulse of 40 msec at −30 mV (holding potential = −100 mV), fit to the equation, $I_{test}/I_{prepulse} = 1 - \exp\{-t/\tau\}$, where t is the time constant of recovery from inactivation, in the absence (○, $n = 4$) and presence (▽, $n = 4$) of ATX II (100 nM. (*H*) Normalized conductance-voltage for hH1 in presence (▽, $n = 5$) and in absence (○, $n = 3$) of ATX II, fitted with a Boltzmann equation.

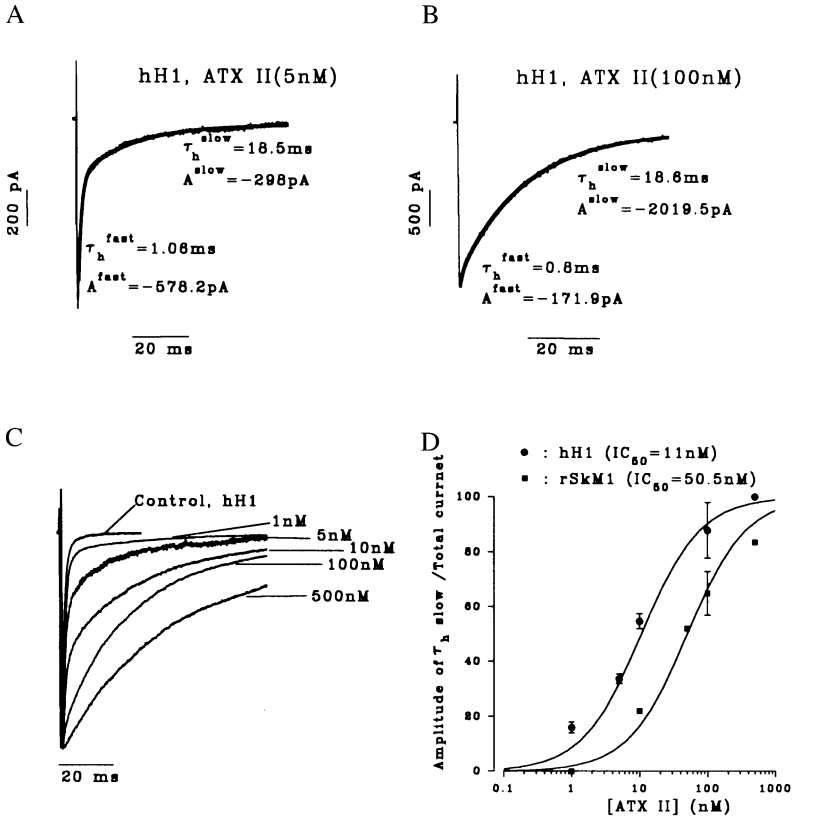

Fig. 4. Dose-response effect of sea anemone toxin (ATX II)-induced slow inactivation of human heart sodium channels (hH1). Current traces obtained a −30 mV voltage steps in presence of 5 nM (*A*) and 100 nM (*B*) and a superimposed two exponential fit of the time course of inactivation, τ_h^{fast} and τ_h^{slow} represent respectively the fast and slow time constants and A^{fast} and A^{slow} represent respectively the amplitudes of the fast and the slow component. (*C*) Effect of various concentrations of ATX II on hH1 sodium currents recorded at −20 mV, stepped from a holding potential of −140 mV. (*D*) The ratio of τ_h^{slow} relative amplitude to the peak current amplitude at −20 mV of hH1 and rSkM1 is plotted against ATX II concentration (holding potential is −140 mV), each data point represent a mean ± SEM of 3 to 4 experiments.

II dramatically disrupts the gating of single sodium channels (Fig. 5*B* and *D* compared with 5*A* and *C*): the mean open times measured at a test voltage of −20 mV were increased 2-fold (0.49 ± 0.02 msec (n = 3) without and 0.99 ± 0.04 msec (n = 3) with of 1,000 nM ATX II). However, our data show that ATX II has no effect on the single channel current amplitudes suggesting that the toxin does not affect the conductance of the sodium channels (Fig. 5*E*). This is consistent with the value of the conductance obtained from the limiting slope of *I-V* curves of the single channel data (22.3 pS) and is comparable with the conductance found for hH1 expressed in *Xenopus* oocytes.

Effects of ATX II on hSkM1

We also expressed the human homologue of rSkM1, hSkM1, in the tsA201 cell line and compared the kinetics changes of sodium channels with those treated with 100 nM ATX II. Similar results were obtained as for the rSkM1 isoform (Fig. 6). ATX II at 100 nM induced a slowing of inactivation rate (τ_h^{slow}) by a factor of 12-fold at −20 mV.

ATX II Induce an Inward Residual Current

An interesting feature of the action of ATX II on hH1 and rSkM1 (also hSkM1, *data not shown*) is that in the presence of toxin a residual or window current (I_{res}) appears (Fig. 7). This residual current is not related to linear currents since despite using a P/4 procedure, the current remains (*data not shown*). Single channels from hH1 were also recorded using a long pulse protocol (Fig. 7*C*). The ensemble averages of single channel currents of this patch, shows that this residual current is related to late sodium channel openings (Fig. 7*D*).

Discussion

Sea anemone (*Anemonia sulcata*) nematocysts contain several active polypeptide toxins, including ATX II, which are used to capture sea prey by altering the function of toxin-sensitive voltage-sensitive sodium channels. ATX II shows greater specificity for cardiac than skeletal muscle or brain voltage-gated sodium channels and consists of 47 amino acids containing three disulfide bridges (Béress et al., 1975*a*,*b*). This toxin prolongs the cardiac action potential duration mainly by slowing the inactivation of voltage-gated sodium channels leading to death (Romey et al., 1980; Erxleben & Rathmayer, 1984).

The aim of this study is to characterize the effect of ATX II on cloned sodium channels using whole cell and single channel recording to establish a foundation for

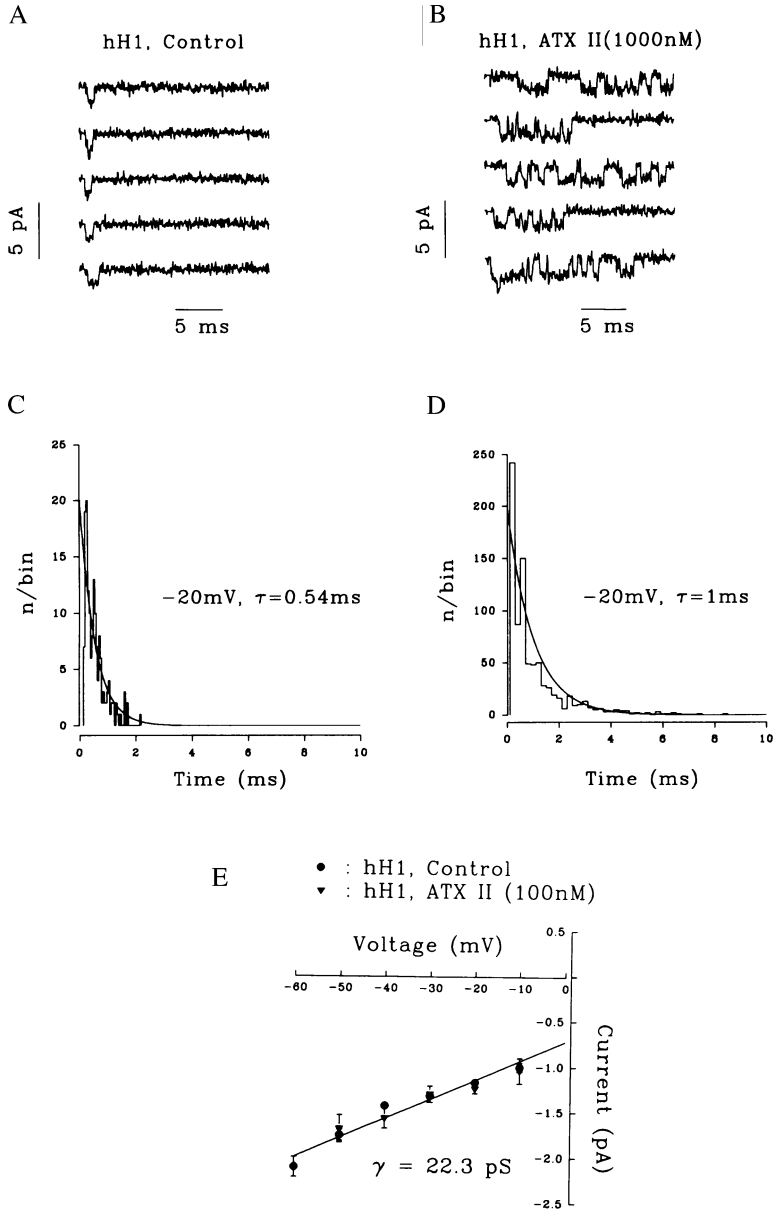

Fig. 5. Effects of sea anemone toxin (ATX II) on human heart (hH1) single channel currents. Single channel currents from cell-attached patches of hH1 expressed in tsA201 cells without (*A*) and with ATX II = 1,000 nM (*B*) at −20 mV depolarizations from a holding potential of −120 mV. In *C* and *D* open time histogram distribution fitted with a single exponential without (*C*) and with (*D*) 1,000 nM ATX II. (*E*) Single channel current-voltage relationship in the absence (●) and presence (▼). The linear regression represented by a solid line has a slope of 22.3 pS. Each data point represents a mean of 5 to 6 measurements.

analysis of its binding site and to determine its mechanism of action. We have employed recombinant human heart (hH1), rat skeletal muscle (rSkM1) and human skeletal muscle (hSkM1) sodium channels which were previously cloned and characterized by expression in *Xenopus* oocytes (Trimmer et al., 1989; Gellens et al., 1992; George et al., 1992; Wang et al., 1992). ATX II dramatically slows hH1 inactivation but shows little effect on channel activation. For both rSkM1 and hH1 at high concentrations of toxin, the kinetics of inactivation is a single exponential process: at intermediate concentrations of toxin, the inactivation phase becomes complex exhibiting a biexponential character due to the simultaneous existence of free and toxin-bound channels which are represented by current decay time constants τ_h^{fast} and τ_h^{slow}, respectively. For hH1 the slope of the voltage-dependence of inactivation is near zero or, possibly, reversed with τ_h^{slow} values increasing with greater depolarization at voltages more positive than −30 mV. This suggests that ATX II reduces the rate of inactivation from open states such that more inactivation occurs from closed states. Our single channel data agree with this interpretation revealing increases of twofold in the mean open times in the presence of toxin, consistent with a decrease in the rate of transition from open to inactivated state (Aldrich, Corey & Stevens, 1983; Vandenberg & Horn, 1984). An additional contribution to the slower inactivation seen in the macroscopic currents is channel reopening in the presence of toxin which is seen in the single-channel data (Fig. 5*B*). ATX II has similar effects

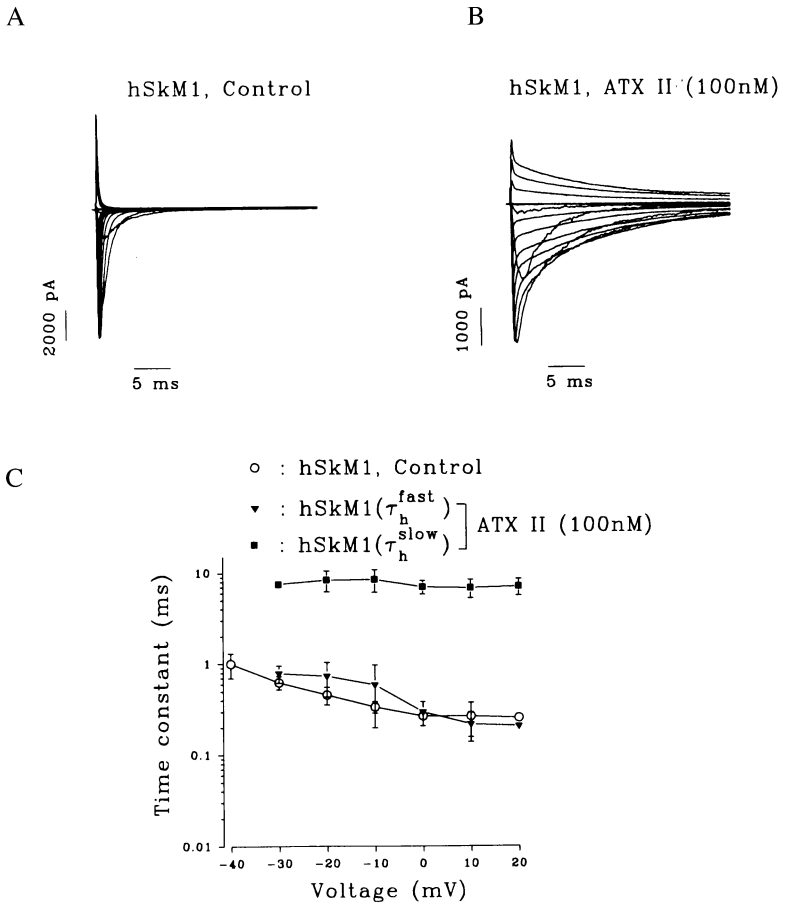

Fig. 6. Effects of sea anemone toxin (ATX II) on human skeletal muscle (hSkM1) sodium channels. (*A*) Whole-cell sodium currents due to hSkM1 sodium channels recorded from transfected tsA201 cell line at a holding potential of −100 mV and stepped from −80 to +60 mV in 10 mV increments: *A* in absence and *B* in presence of 100 nM ATX II. (*B*) Effects of ATX II on the voltage dependence of inactivation of hSkM1. (*C*) As indicated the time constant of inactivation (τ_h) was plotted *vs.* voltage, τ_h for monophasic kinetics in absence (○, $n = 3$) of ATX II and τ_h^{fast} (▼, $n = 3$) and τ_h^{slow} (■, $n = 3$) for biphasic kinetics in the presence of ATX II.

on rSkM1 and hSkM1 although these effects require higher toxin concentrations. Thus, in agreement with other studies performed on native tissues our results on recombinant channel α-subunits indicate that (i) ATX II slows inactivation of sodium channels with no detectable effect on activation and (ii) hH1 (IC_{50} = 11 nM) is ~5-fold more sensitive to this toxin than rSkM1 (IC_{50} = 51 nM) expressed in tsA201 cells (Fig. 3*B*). The cardiac and skeletal muscles subtypes must have somewhat different structures in terms of the ATX II binding site and/or are different in the manner by which the effect of occupancy of the toxin binding site is transduced to the other parts of the channel during inactivation. Classical theory attributes the opening and closing of voltage-gated sodium channels to charged particles or ''gates'': m-gates for activation and a h-gates for inactivation (Hodgkin & Huxley, 1952). The h-gate, visualized as a ''ball and chain'' (Armstrong & Bezanilla, 1977) or ''hinged lid,'' is localized on the cytoplasmic surface associated with the interdomain 3–4 loop (West et al., 1992). Although the toxin may be acting allosterically with the h-gate or its receptor, an equally plausible possibility is that it operates on a voltage-sensor involved in inactivation. Recent evidence involving positive-charge-reducing mutations in S4 helices in all domains implicates a unique role for S4 of Domain 4 (D4) in inactivation (Chen et al., 1995). This extends observations on naturally occurring inactivation-impaired sodium channel α-subunits seen in some patients with periodic paralysis involving mutations at the extracellular surface in D4 (Chahine et al., 1994). It is of interest that two Familial Hyperkalemic Periodic Paralysis (FHPP) mutations, M1585V and T698M, located near the putative cytoplasmic surface of the channel show residual currents and that this pathophysiology can be mimicked by ATX II treatment of wild-type channels in rat muscle fibers (Cannon & Corey, 1993; Cannon & Strittmatter, 1993). This is reminiscent of the persistent residual current (I_{res}), lasting to the end of the test pulse, recorded for rSkM1, hH1 and hSkM1 (*data not shown*) isoforms in the presence of ATX II (Fig. 7*A* and *B*). Our data suggest (Fig. 7*C* and *D*) that the residual current of hH1 observed in presence of ATX II is related to late openings of single sodium channels. Also high concentration of TTX (50 μM) reduce considerably the amplitude of the residual current (*data not shown*).

Neither the reversal potential nor the conductance the ATX II-treated channels is altered suggesting that the

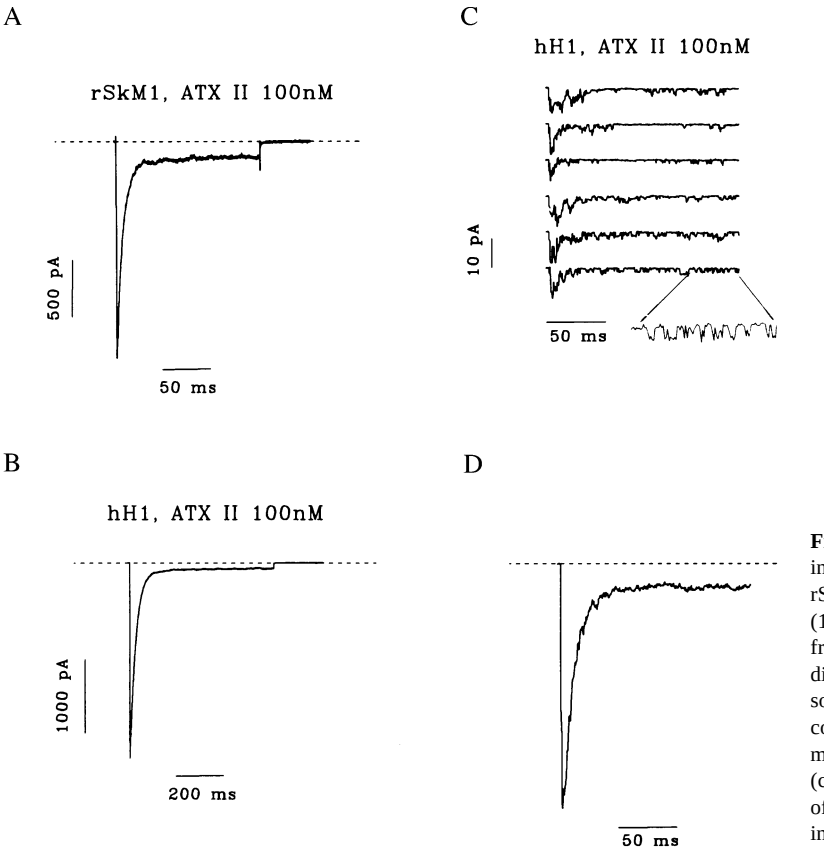

Fig. 7. Sea anemone toxin (ATX II) induce an inward residual current. Residual currents of rSkM1 (*A*) and hH1 (*B*) in the presence of ATX II (100 nM). Sodium currents recorded at −30 mV from a holding potential of −100 mV. Note difference in time scales. (*C*) Selected traces of sodium channels currents obtained in cell attached configuration, with several active channels at −20 mV test pulse in presence of 1,000 nM ATX II (currents filtered at 2 KHz). (*D*) Ensemble average of 100 traces, showing the residual current of hH1 in presence of ATX II.

toxin has no effect on the selectivity filter or on the ion permeation pathway of the channel, perhaps because its binding site is too distant.

Another two-pulse protocol was used to assess the effect of the toxin on the recovery from inactivation. In the presence of the toxin, the recovery from inactivation is faster, once again suggesting that the inactivation state was destabilized. Slowing of the kinetics of inactivation and increasing the rate of recovery from inactivation are also seen with PC mutations, R1448C or R1448H, located on the putative external side of the channel in the S4 voltage-sensing element of D4 (Chahine et al., 1994).

Future experiments will be directed toward identifying the structural differences between skeletal muscle (rSkM1 and hSkM1) and cardiac muscle (hH1) responsible for the variation that these sodium channel subtypes exhibit in terms of their sensitivities to ATX II and the detailed mechanisms of toxin action.

The authors thank Dr. R. Horn for helpful discussions. The work was supported by the Medical Research Council of Canada MT-12554 (MC), Heart and Stroke Foundation of Canada (MC), the American Heart Association, Muscular Dystrophy Foundation, Research Foundation of the University of Pennsylvania and NIH Grant AR 41,762 (R.G.K.). M. Chahine is Research Scholar of the Heart and Stroke Foundation of Canada.

References

Aldrich, R.W., Corey, D.P., Stevens, C.F. 1983. A reinterpretation of mammalian sodium channel gating based on single channel recording. *Nature* **306:**436–441

Alsen, C., Harris, J.B., Tesseraux, I. 1981. Mechanical and electrophysiological effects of sea anemone (*Anemonia sulcata*) toxins on rat innervated and denervated skeletal muscle. *Br. J. Pharmacol.* **74:**61–71

Armstrong, C.M., Bezanilla, F. 1977. Inactivation of the sodium channel. II. Gating current experiments. *J. Gen. Physiol.* **70:**567–590

Backx, P.H., Yue, D.T., Lawrence, J.H., Marban, E., Tomaselli, G.F. 1992. Molecular localization of an ion-binding site within the pore of mammalian sodium channels. *Science* **257:**248–251

Béress, L., Béress, R., Wunderer, G. 1975*a*. Isolation and characterization of three polypeptides with neurotoxic activity from *Anemonia sulcata*. *FEBS Lett.* **50:**311–314

Béress, L., Béress, R., Wunderer, G. 1975*b*. Purification of three polypeptides with neuro- and cardiotoxic activity from the sea anemone *Anemonia sulcata*. *Toxicon* **13:**359–367

Blair, R.W., Peterson, D.F., Bishop, V.S. 1978. The effects of anthopleurin-A on cardiac dynamics in conscious dogs. *J. Pharmacol. Exp. Ther.* **207:**271–276

Cannon, S.C., Corey, D.P. 1993. Loss of Na^+ channel inactivation by anemone toxin (ATX II) mimics the myotonic state in hyperkalaemic periodic paralysis. *J. Physiol.* **466:**501–520

Cannon, S.C., Strittmatter, S.M. 1993. Functional expression of sodium channel mutations identified in families with periodic paralysis. *Neuron* **10:**317–326

Catterall, W.A. 1992. Cellular and molecular biology of voltage-gated sodium channels. *Physiol. Rev.* **72:**S15–S48

Catterall, W.A. 1994. Structure and modulation of Na^+ and Ca^{2+} channels. *Ann. N.Y. Acad. Sci.* **707:**1–19

Chahine, M., Bennett, P.B., George, A.L., Jr., Horn, R. 1994. Functional expression and properties of the human skeletal muscle sodium channel. *Pfluegers Arch.* **427:**136–142

Chahine, M., Chen, L.-Q., Fotouhi, N., Walsky, R., Fry, D., Samtarelli, V., Horn, R., Kallen, R.G. 1995. Characterizing the μ-conotoxin binding site on voltage-sensitive sodium channels with analogs and channels mutations. *Receptors & Channels* **3:**161–174

Chahine, M., George, A.L., Jr., Zhou, M., Ji, S., Sun, W., Barchi, R.L., Horn, R. 1994. Sodium channel mutations in paramyotonia congenita uncouple inactivation from activation. *Neuron* **12:**281–294

Chen, L.-Q., Chahine, M., Kallen, R.G., Barchi, R.L., Horn, R. 1992. Chimeric study of sodium channels from rat skeletal and cardiac muscle. *FEBS Lett.* **309:**253–257

Chen, L.-Q., Santarelli, V., Zhang, P., Horn, R., Kallen, R.G. 1995. Unique role for the S4 segment of domain 4 of sodium channels. *Biophys. J.* **68:**A156

El-Sherif, N., Fozzard, H.A., Hanck, D.A. 1992. Dose-dependent modulation of the cardiac sodium channel by sea anemone toxin ATXII. *Circ. Res.* **70:**285–301

Erxleben, C., Rathmayer, W. 1984. Effects of the sea anemone *Anemonia sulcata* toxin II on skeletal muscle and on neuromuscular transmission. *Toxicon* **22:**387–399

Frelin, C., Vigne, P., Schweitz, H., Lazdunski, M. 1984. The interaction of sea anemone and scorpion neurotoxins with tetrodotoxin-resistant Na^+ channels in rat myoblasts. A comparison with Na^+ channels in other excitable and non-excitable cells. *Mol. Pharmacol.* **26:**70–74

Gellens, M.E., George, A.L., Jr., Chen, L., Chahine, M., Horn, R., Barchi, R.L., Kallen, R.G. 1992. Primary structure and functional expression of the human cardiac tetrodotoxin-insensitive voltage-dependent sodium channel. *Proc. Natl. Acad. Sci. USA* **89:**554–558

George, A.L., Jr., Komisarof, J., Kallen, R.G., Barchi, R.L. 1992. Primary structure of the adult human skeletal muscle voltage-dependent sodium channel. *Ann. Neurol.* **31:**131–137

Hille, B. 1992. Ionic Channels of Excitable Membranes. Sinauer Associates, Sunderland, MA

Hodgkin, A.L., Huxley, A.F. 1952. A quantitative description of membrane current and its application to conduction and excitation in nerve. *J. Physiol.* **117:**500–544

Horn, R., Lange, K. 1983. Estimating kinetic constants from single channel data. *Biophys. J.* **43:**207–223

Kallen, R.G., Cohen, S.A., Barchi, R.L. 1993. Structure, function and expression of voltage-dependent sodium channels. *Mol. Neurobiol.* **7:**383–428

Krafte, D.S., Davison, K., Dugrenier, N., Estep, K., Josef, K., Barchi, R.L., Kallen, R.G., Silver, P.J., Ezrin, A.M. 1994. Pharmacological modulation of human cardiac Na^+ channels. *Eur. J. Pharmacol.* **266:**245–254

Lipkind, G.M., Fozzard, H.A. 1994. A structural model of the tetrodotoxin and saxitoxin site of the Na^+ channel. *Biophys. J.* **66:**1–13

Margolskee, R.F., McHendry-Rinde, B., Horn, R. 1993. Panning transfected cells for electrophysiological studies. *Biotechniques* **15:**906–911

Noda, M. 1994. Structure and function of sodium channels. *Ann. N.Y. Acad. Sci.* **707:**20–37

Noda, M., Shimizu, S., Tanabe, T., Takai, T., Kayano, T., Ikeda, T., Takahashi, H., Nakayama, H., Kanaoka, Y., Minamino, N., Kangawa, K., Matsuo, H., Raftery, M.A., Hirose, T., Inayama, S., Hayashida, H., Miyata, T., Numa, S. 1984. Primary structure of *Electrophorus electricus* sodium channel deduced from cDNA sequence. *Nature* **312:**121–127

Ptácek, L.J., George, A.L., Jr., Barchi, R.L., Griggs, R.C., Riggs, J.E., Robertson, M., Leppert, M.F. 1992. Mutations in an S4 segment of the adult skeletal muscle sodium channel cause paramyotonia congenita. *Neuron* **8:**891–897

Romey, G., Renaud, J.F., Fosset, M., Lazdunski, M. 1980. Pharmacological properties of the interaction of a sea anemone polypeptide toxin with cardiac cells in culture. *J. Pharmacol. Exp. Ther.* **213:**607–615

Satin, J., Kyle, J.W., Chen, M., Bell, P., Cribbs, L.L., Fozzard, H.A., Rogart, R.B. 1992. A mutant of TTX-resistant cardiac sodium channels with TTX-sensitive properties. *Science* **256:**1202–1205

Schreibmayer, W., Kazerani, H., Tritthart, H.A. 1987. A mechanistic interpretation of the action of toxin II from *Anemonia sulcata* on the cardiac sodium channel. *Biochim. Biophys. Acta* **901:**273–282

Shibata, S., Norton, T.R., Izumi, T., Matsuo, T., Katsuki, S. 1976. A polypeptide (AP-A) from sea anemone (*Anthopleura xanthogrammica*) with potent positive inotropic action. *J. Pharmacol. Exp. Ther.* **199:**298–309

Terlau, H., Heinemann, S.H., Stühmer, W., Pusch, M., Conti, F., Imoto, K., Numa, S. 1991. Mapping the site of block by tetrodotoxin and saxitoxin of sodium channel II. *FEBS Lett.* **293:**93–96

Thomsen, W.J. Catterall, W.A. 1989. Localization of the receptor site for α-scorpion toxins by antibody mapping: implications of sodium channel topology. *Proc. Natl. Acad. Sci. USA* **86:**10161–10165

Torda, A.E., Mabbutt, B.C., Van Gunsteren, W.F., Norton, R.S. 1988. Backbone folding of the polypeptide cardiac stimulant anthopleurin-A determined by nuclear magnetic resonance, distance geometry and molecular dynamics. *FEBS Lett.* **239:**266–270

Torda, A.E., Norton, R.S. 1989. Proton NMR relaxation study of the dynamics of anthopleurin-A in solution. *Biopolymers* **28:**703–716

Trimmer, J.S., Cooperman, S.S., Tomiko, S.A., Zhou, J., Crean, S.M., Boyle, M.B., Kallen, R.G., Sheng, Z., Barchi, R.L., Sigworth, F.J., Goodman, R.H., Agnew, W.S., Mandel, G. 1989. Primary structure and functional expression of a mammalian skeletal muscle sodium channel. *Neuron* **3:**33–49

Vandenberg, C.A., Horn, R. 1984. Inactivation viewed through single sodium channels. *J. Gen. Physiol.* **84:**535–564

Vincent, J.P., Balerna, M., Barhanin, J., Fosset, M., Lazdunski, M. 1980. Binding of sea anemone toxin to receptor sites associated with gating system of sodium channel in synaptic nerve endings in vitro. *Proc. Natl. Acad. Sci. USA* **77:**1646–1650

Wang, J., Rojas, C.V., Zhou, J., Schwartz, L.S., Nicholas, H., Hoffman, E.P. 1992. Sequence and genomic structure of the human adult skeletal muscle sodium channel a subunit gene on 17q. *Biochem. Biophys. Res. Commun.* **182:**794–801

West, J.W., Patton, D.E., Scheuer, T., Wang, Y., Goldin, A.L., Catterall, W.A. 1992. A cluster of hydrophobic amino acid residues required for fast Na^+-channel inactivation. *Proc. Natl. Acad. Sci. USA* **89:**10910–10914

White, M.M., Chen, L., Kleinfield, R., Kallen, R.G., Barchi, R.L. 1991. SkM2, a Na^+ channel cDNA clone from denervated skeletal muscle, encodes a tetrodotoxin-insensitive Na^+ channel. *Mol. Pharmacol.* **39:**604–608

Widmer, H., Billeter, M., Wuthrich, K. 1989. Three dimensional structure of the neurotoxin ATX Ia from *Anemonia sulcata* in aqueous solution determined by nuclear magnetic resonance spectroscopy. *Proteins* **6:**357–371

Wilcox, G.R., Fogh, R.H. Norton, R.S. 1993. Refined structure in solution of the sea anemone neurotoxin ShI. *J. Biol. Chem.* **268:**24707–24719